

Corrosion of mild steel and 316L austenitic stainless steel with different surface roughness in sodium chloride saline solutions

L. Abosrra, A. F. Ashour, S. C. Mitchell & M. Youseffi
School of Engineering, University of Bradford, UK

Abstract

The corrosion behaviour of mild steel and 316L austenitic stainless steel was investigated in saline solution containing 1 and 3%NaCl. Specimens with surface roughness of 200, 600 grit emery paper and 1 μ m diamond paste were investigated. The anodic polarization measurement technique was performed at a scan rate of 1mV/s for a fixed period of 1 hour. The experimental results revealed that chloride ions have a significant effect on the corrosion behaviour of both steels as expected. As the surface roughness of 316L stainless steel increased, the breakdown potential (E_{break}), the free corrosion potential (E_{corr}) and the width of passivity decreased, hence the corrosion rate increased. However, in the case of mild steel specimens, improving surface finish lead to shifts in the corrosion potential to more noble states and increased the corrosion rate. Metallographic examination of corroded specimens after electrochemical corrosion tests confirmed that the breakdown of the passive region was due to pitting corrosion.

Keywords: mild steel, 316L SS, anodic polarization, corrosion, surface roughness, saline solution.

1 Introduction

The study of corrosion properties of mild steel and stainless steel in aqueous solutions has received a great general attention. Mild steel is the most common structural material and is used in a wide range of environments. It is well known that when mild steel corrodes, anodic and cathodic areas develop over the corroded surface. Conventionally, these pits are known to change in shape and move across the surface, resulting in early corrosion that is approximately



uniform [1]. However, when mild steel is exposed to saline solutions and a marine environment this type of corrosion is not observed. Anodic regions and micro-pits develop very quickly after early exposure and the further presence of shallow broad pits occurs [2, 3]. When a high corrosion resistance is required, stainless steel is recommended. Type 316L stainless steel is austenitic and has been used in the chemical and petrochemical industries and offshore structures for many decades. The excellent corrosion resistance of this stainless steel is attributed to the formation of a stable passive oxide layer, but nevertheless stainless steel is susceptible to localized corrosion by chloride ions [4]. In addition to choosing the right stainless steel grade for good corrosion resistance, it is equally important to specify the right surface condition of the materials used in many applications [5]. The surface condition affects the corrosion resistance to a certain extent, which implies that it is possible to meet certain requirements by specifying the proper finish rather than upgrading the chosen alloy. The effect of surface condition on corrosion resistance of 301, 304L and duplex stainless steel has been documented elsewhere [6–8]. Since the pitting potential actually defines a minimum condition under which pits can become stable, the aim is to lower the pitting potential. Metastable pitting occurs throughout the passive region of stainless steel and the potential at which the transition to stable pit growth occurs is an important parameter describing the stability of the metal [6, 9, 10]. In this study the effect of surface roughness on the corrosion resistance of mild steel and 316L austenitic stainless steel in the presence of different chloride concentrations was investigated using the electrochemical technique. Corrosion parameters, such as the breakdown potential, the free corrosion potential, and the corrosion rate, were determined.

2 Experimental methods

2.1 Sample preparation

The chemical compositions are given in weight % for mild steel as: 0.84 Mn, 0.53 Cu, 0.24 Si, and 0.19 C and for 316L stainless steel as: 18Cr, 14 Ni, 2.0 Mn, 0.75 Si, 0.03 C and 0.27 Mo. Corrosion tests were performed on cylindrical specimens with 9.5mm diameter and 12.8mm length with an exposed area of 4.5cm². Specimen surfaces roughness was generated by wet grinding using silicon carbide papers of 200 and 600 grits and the polished surface was generated using 1µm diamond paste.

2.2 Electrochemical measurements

Electrochemical tests were carried out in saline solutions containing 1 and 3% NaCl using the standard electrochemical corrosion cell containing three electrodes: the saturated calomel electrode (SCE), the counter electrode (graphite) and the working electrode (the sample). All electrodes were immersed in a suitable glass vessel containing 600ml of the saline electrolyte. The anodic and cathodic polarization curves were measured after 1hr of working electrode



immersion at ambient temperature ($23 \pm 2^\circ\text{C}$) in the investigated environment. Subsequently, the anodic polarization curves for both mild steel and 316L stainless steel were measured from potential values below and above the free corrosion potentials of $\pm 250 \text{ mV } E_{corr}$ and $\pm 800 \text{ mV}$, respectively, with a scan rate of 1 mV/sec .

The experiments were repeated 3-4 times for all specimens in all solutions. Corrosion rates were calculated for steel immersed in aqueous solutions using eqn. (1) [11].

$$CR = \frac{0.13 I_{Corr} W}{DA} \quad (1)$$

where I_{Corr} = corrosion current density ($\mu\text{A}/\text{cm}^2$), W = Atomic weight of steel, D = Density of steel in gm/cm^3 , and A is the exposed surface area of the steel in cm^2 .

3 Results

3.1 Electrochemical data analysis

3.1.1 Mild steel – potentiodynamic results

Figure 1 gives the potentiodynamic polarization curves of mild steel with surface roughness of 200 and 600 grit papers as well as $1\mu\text{m}$ diamond paste polished surface tested in 1% NaCl solution. The corrosion behaviour was affected by the degree of surface roughness. An increase in roughness from polishing (like mirror) to 600 and 200 grit surface roughness shifted the free corrosion potential to more active values as shown in Figures 1 and 3. The corrosion rate values were not expressing the same trend recorded for the free corrosion potential. A specimen of diamond polished surface showed a higher corrosion rate than the 600 and 200 grit surface finished specimens as shown in Figure 4. Figure 2 shows the corrosion behaviour of $1\mu\text{m}$ diamond polished (like mirror), 600 and 200 grit surface roughness mild steel specimens in 3% NaCl saline solution. Corrosion resistance was drastically reduced with increasing sodium chloride concentration up to 3%. Figure 3 indicated that as the surface became rougher the free corrosion potential moved to a more active state. Corrosion rate measurements showed contradictory results and the conventional trend is that increasing the surface roughness decreases corrosion resistance. The specimens with diamond polished surfaces had the highest corrosion rate as illustrated in Figure 4.

3.1.2 Stainless steel (316L) – potentiodynamic results

Potentiodynamic polarization curves and the retrieved corrosion data for 316L stainless steel in 1% and 3% NaCl are shown in Figures 5–9. The polarization curves shown in Figures 5 and 6 indicated that the tendency of the stainless steel



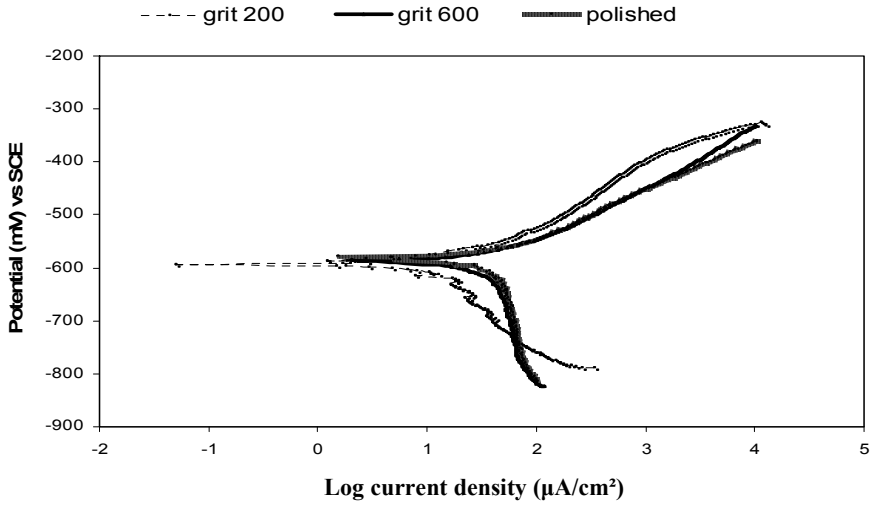


Figure 1: Polarization curves of mild steel at different surface roughness in 1% NaCl saline solution.

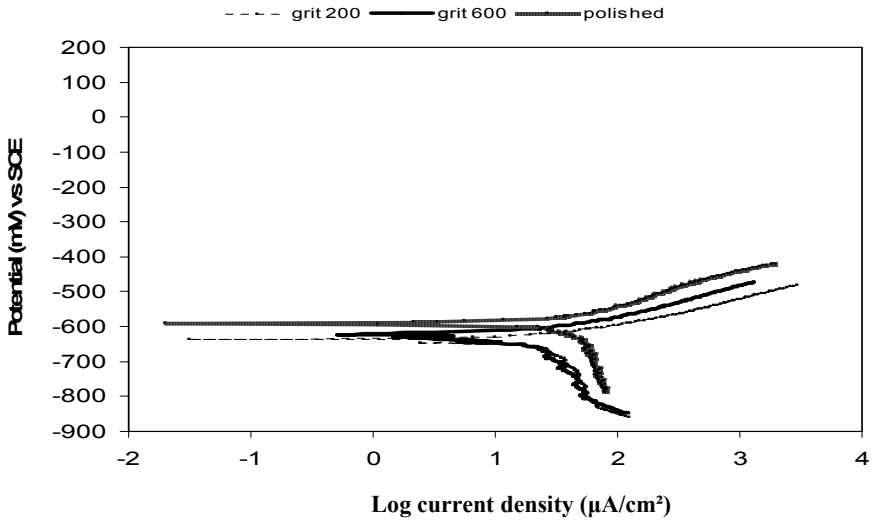


Figure 2: Polarization curves of mild steel at different surface roughness in 3% NaCl saline solution.

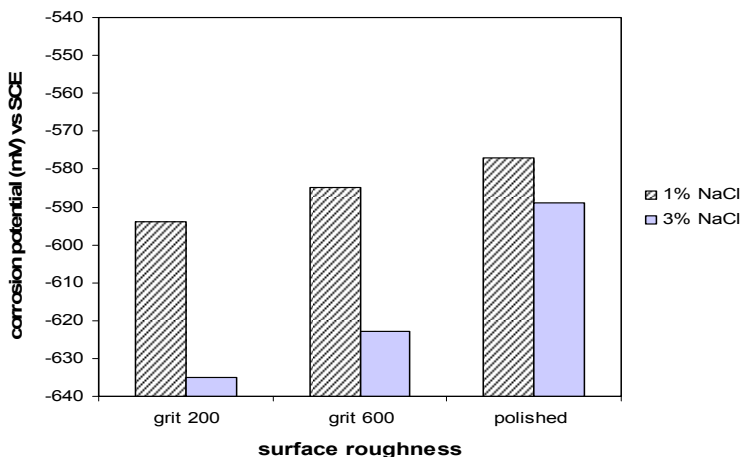


Figure 3: Corrosion potential vs. surface roughness in 1% and 3% NaCl saline solution.

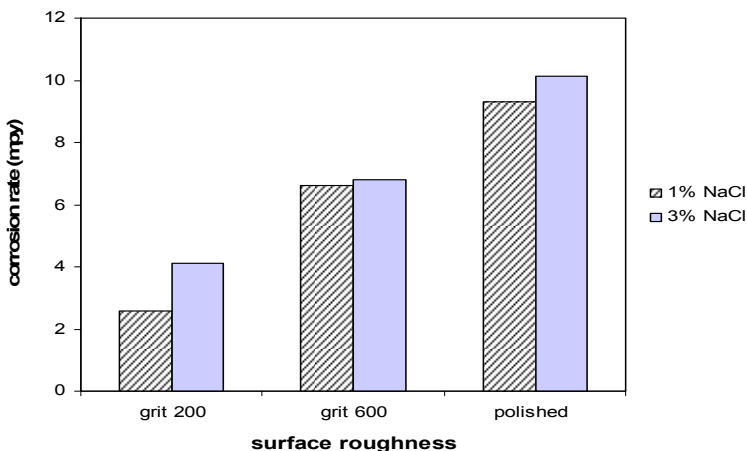


Figure 4: Corrosion rate vs. surface roughness in 1% and 3% NaCl saline solution.

was to undergo oxidation and passivation, followed by breakdown, i.e. a typical characteristic. The polarization curve of specimens with surface finishes of $1\mu\text{m}$ diamond polish, 600 and 200 grit papers tested in 1% NaCl saline solution is shown in Figure 5. The passivity and hence the breakdown potential was affected by the surface roughness. Specimen with less roughness, i.e. $1\mu\text{m}$ diamond finish surface, had the highest breakdown potential of +317 mV, followed by 600 and 200 grit surface roughness specimens. The passivity of rougher surfaces of 200 and 600 grit failed at less noble potentials of +286 mV and +296 mV,

respectively. Figure 6 shows the corrosion behaviour of specimens tested in 3% NaCl. The polarization curves of the investigated specimens showed the conventional trend of the effect of chlorides and surface roughness. As the chloride concentration and the surface roughness increased, the breakdown potential values decreased and the free corrosion potential moved in a more

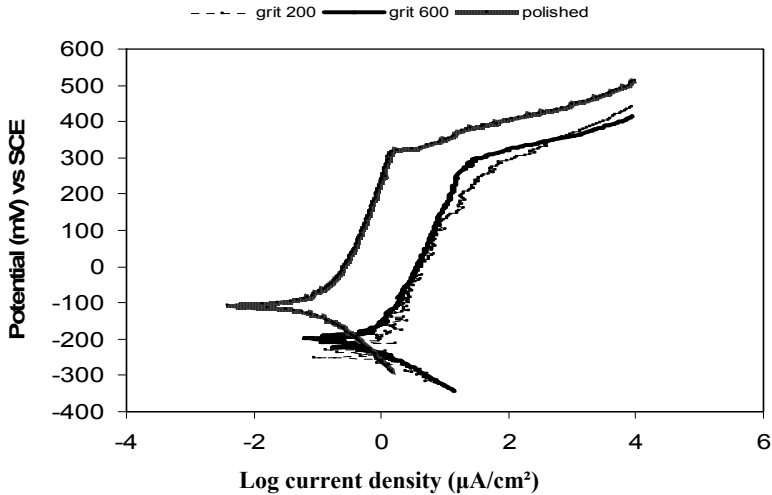


Figure 5: Polarization curves for different surface roughness of 316L stainless steel in 1% NaCl saline solution.

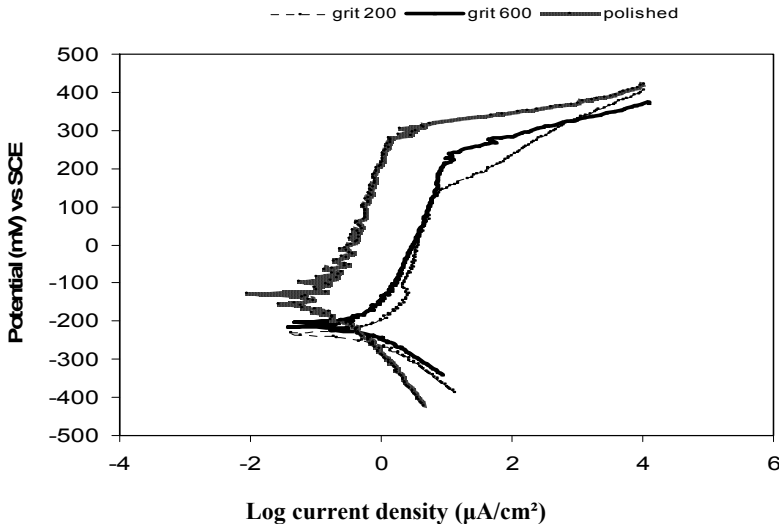


Figure 6: Polarization curves for different surface roughness of 316L stainless steel in 3% NaCl saline solution.

active direction (less stable). The free corrosion potentials, breakdown potentials and corrosion rates in 1 and 3% NaCl were recorded and displayed in Figures 7–9. Figure 7 shows that for the same surface finish specimen, the free corrosion potential increased to a more noble state as the surface roughness decreased. The chloride concentration had a significant effect and reduced the free corrosion potential as the NaCl content increased from 1 to 3%. Figures 8 and 9 show the breakdown potential and the corrosion rate results, respectively.

3.2 Morphology results

Corroded specimens after testing were investigated at low and high magnifications for microscopy studies. Examples of mild steel specimen corrosion morphology are shown in Figure 10. Figure 10(a) shows the corrosion pits on the mild steel specimen of diamond polished surface tested in 3% NaCl. This figure shows clearly the severity of the corrosion damage and this confirms and justifies the reason for the highest corrosion rate values recorded for this specimen. Corrosion on 200 grit paper surface roughness tested in 3% NaCl shown in Figure 10(b) clearly reveals a cluster of less deep pitting corrosion, as indicated by the white arrows. Corrosion morphology on 316L stainless steel specimens was investigated using the scanning electron microscope (SEM). The results are shown in Figure 11. Figure 11(a) shows several open corrosion pits on the surface of the 200 grit specimen. The pitting corrosion morphology transformed to another type, called lacelike corrosion pits, as the surface became smoother as can be seen in Figure 11(b). These types of corrosion pits are due to

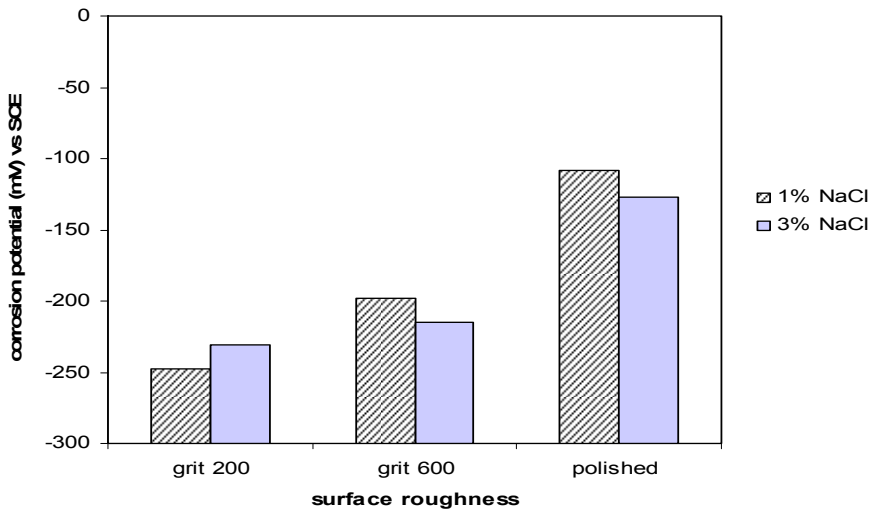


Figure 7: Corrosion potential of 316L stainless steel with various surface roughness in 1% and 3% NaCl saline solution.

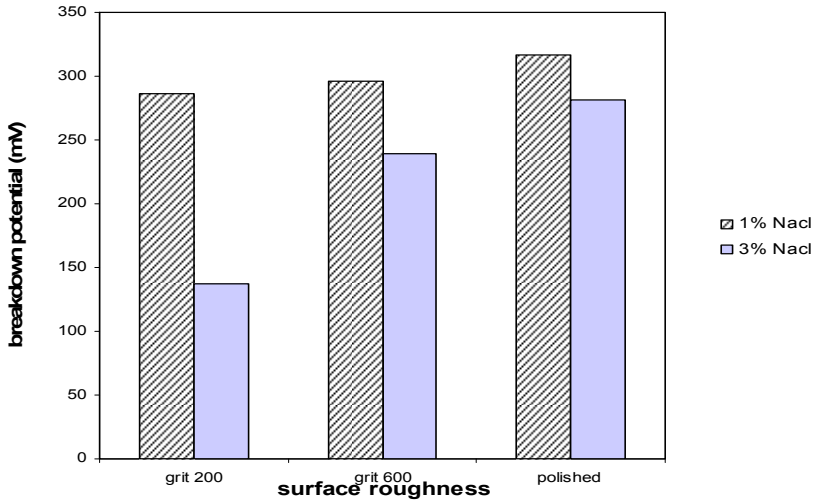


Figure 8: Breakdown potential of 316L stainless steel with various surface roughness in 1% and 3% NaCl saline solution.

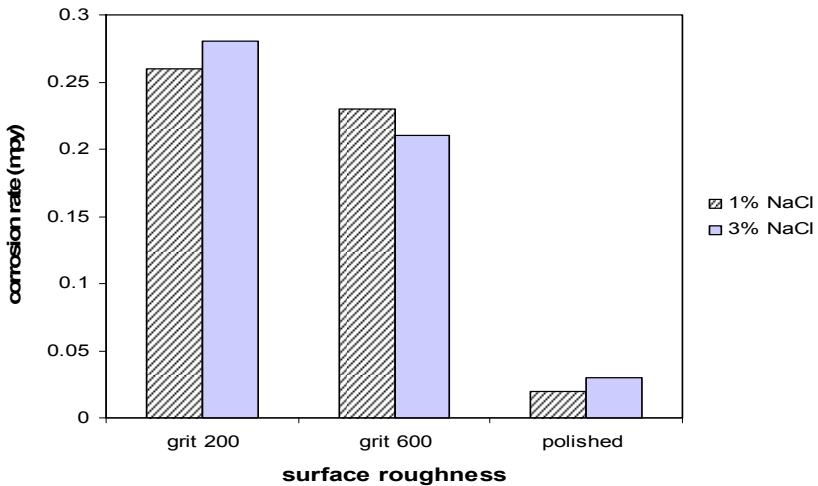


Figure 9: Corrosion rate of 316L stainless steel with various surface roughness in 1% and 3% NaCl saline solution.

the collapse of passive film during pit propagation. The specimen of polished surface, Figure 11(c), showed a high number of lacelike corrosion pits. The corrosion morphology shows that the lacelike corrosion is propagated by the mechanism of diffusion until the final collapse, where the pit became stable.

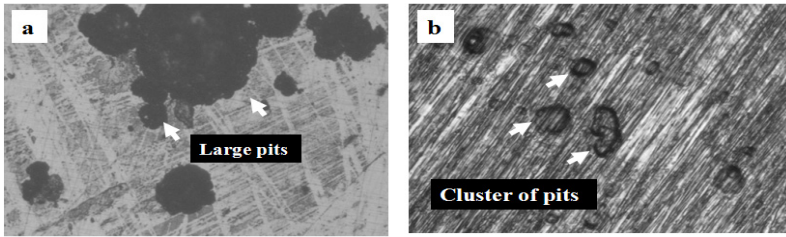


Figure 10: Optical photographs (X400) of corrosion pits on mild steel surfaces: (a) polished grit and (b) 200 grit in 3% NaCl saline solution.

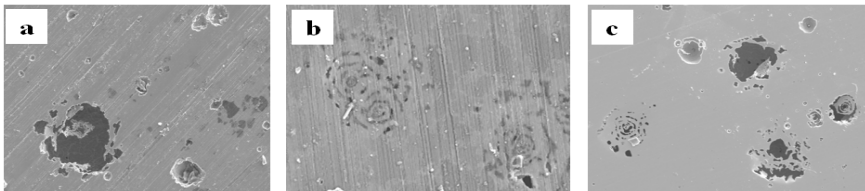


Figure 11: SEM images (X300): (a) 200, (b) 600 grit surface roughness specimens and (c) diamond polished specimen, respectively.

4 Discussion

Mild steel initially showed some weak passivation range and, due to the presence of chloride on the vicinity of the steel surface, the passivity was easily destroyed. At the end of each experiment on mild steel samples, localized corrosion and red rust was visually observed, indicating corrosion attack and products of various kinds due to the presence of aggressive chloride ions, which are a powerful oxidizing agent and combine rapidly with the metal forming metal chloride. Polarization curves revealed weak passivation when sodium chloride increased from 1 to 3%. This is due to the absorption of water molecules and chloride ions on the steel surface causing breakdown of the oxide film. Corrosion mechanisms retrieved from these results are in agreement with the interpretation provided by others [12, 13]. Increasing the surface roughness shifted the corrosion potential in a more noble direction; however the corrosion current density decreased. This was attributed to a weak passive film which formed on the metal surface, causing the early breakdown of passivity with more aggressive chloride ions. The interesting result obtained in this work was that mild steel with smooth polished surfaces showed the highest corrosion rate compared with 600 and 200 grit surface finished specimens. This can be attributed to the high rate of corrosion propagation after initiation. Pitting corrosion is controlled by the diffusion process and in this case once the pitting started, it propagated at a fast rate due to the continuous diffusion process and the formation of acid media at the bottom of the pits. The corrosion resistance of stainless steel is attributed to the presence of chromium forming an oxide film and protecting the steel from further

corrosion in the passive region. However, the presence of certain ionic species, such as chloride ions, in the electrolyte can be very aggressive towards the corrosion behaviour. In this study the anodic polarization curves in various chloride concentrations with different surface roughness clearly revealed that the free corrosion potentials and breakdown potential dropped from more noble values to less noble values as sodium chloride increased from 1 to 3%. This is because chloride ions lower the activation energy required for corrosion reaction to occur. This interpretation is in agreement with the work provided by others [14–17]. The chloride formation did not stop the oxide film formation but reduced the passive region as seen in the polarization curves in Figures 5 and 6. There are other reasons for more aggressive behaviour, reflected in the reduction in the passive region in saline solution, which can be due to chloride ions with higher charge density and higher capacity to form soluble species. By entering into the lattice film, the chloride introduces lattice defects, which reduce the resistance of the oxide film to corrosion as seen from the corrosion rate values in Figure 9. The role of surface roughness on the breakdown potential was confirmed as smoother surfaces had a higher breakdown potential. The potentiodynamic results in Figures 5 and 6 showed that the width of the passive region is highly dependent on the surface condition. When the surface finish varied from smooth to rough, the passive film terminated at a lower breakdown potential and the passive region became shorter due to the effect of surface topography, which enhanced the presence of more aggressive corrosion media inside such rough surfaces. The pitting potential is more sensitive to surface roughness changes and the relatively large increase in pitting potential by several tenth mV from the roughest to smoothest surface, suggested that both the nucleation and propagation of metastable pits depends on the steel surface [6]. This implies that for the metastable pit or pits to grow on a smoother surface is more difficult than on a rougher surface and the presence of chloride ions in the solution results in the destruction of the passive film as observed elsewhere [9, 10]. The mechanism of pit growth is autocatalytic by anodic dissolution of the steel, which leads to the introduction of passive metal ions in solution that cause migration of chloride ions. In turn, metal chloride reacts with water causing the pH to decrease where the cathodic reaction is on the surface near the pit mouth. The results in this study confirmed that when the surface is smooth, the pit will survive more due to the formation of lace cover on the pit mouth maintaining the diffusion process. The corrosion morphology for the diamond surface finish behaved in this manner and showed pitting corrosion with lacelike pits as seen in Figure 11.

5 Conclusions

- Corrosion rate measurements of mild steel specimens showed contradictory results with the conventional trend of corrosion reduction as surface roughness increased. The specimens with diamond polished surfaces had the highest corrosion rate compared with 600 and 200 grit surface finished specimens.



- The free corrosion potential, breakdown potential and corrosion rate of 316L stainless steel are chloride concentration dependent. As the chloride concentration increased, the free corrosion potential and the breakdown potential became less noble. The corrosion rate increased as the chloride concentration increased as expected.
- Reduction in the corrosion resistance of the 316L stainless steel is attributed to the destruction of the passive film in the presence of chloride. The roughest surface of 200 grit showed early passivity breakdown at the highest rate of corrosion and lower breakdown potential compared with the rest of the surfaces.

References

- [1] Uhlig, H. and Revie, R., Corrosion and corrosion control, 3rd edition, John Wiley and Sons: New York, 1985.
- [2] Forgeson, B., Southwell, C. & Alexander, A., Corrosion of metals in tropical environments, part 3-underwater corrosion of ten structural steels, *Corrosion*, **16**, pp 105-114, 1960.
- [3] Blekkenhorst, F., Ferrari, G., Wekken, C. & IJsseling, F., Development of high strength low alloy steels for marine applications, Part 1: results of long term exposure tests on commercially available and experimental steels, *British corrosion journal*, **21**, pp 163–176, 1986.
- [4] Congmin, X., Zhang, Y. & Cheng G., Pitting corrosion behaviour of 316L stainless steel in the media of sulphate- reducing and iron – oxidizing bacteria, *Materials characterization*, **245**, pp 245-256, 2007.
- [5] Kold, J., Anne, R. & Moeller B, Influence of various surface conditions on pitting corrosion resistance of stainless steel tubes type EN 1.4404, presented at NACE corrosion, paper 06095, San Diego, 2006.
- [6] Sasaki, K. and Burstein K.T., The generation of surface roughness during slurry erosion- corrosion and its effect on the pitting potential, *corrosion science*, **38**, pp 2111-2120 1996.
- [7] Moayed, M.H., Laycock, N.J. & Newman, R.C., Dependence of the critical pitting temperature on surface roughness, *corrosion science*, **45**, pp 1203-1216, 2003.
- [8] Elhoud, A., Renton, N.C. & Deans, W.F., Effect of surface roughness on pitting corrosion of 25 Cr duplex stainless steel in chloride solution. The 9th Libyan corrosion conference, Tripoli-Libya, 2007.
- [9] Hong, T. & Nagumo M., Effect of surface roughness on early stages of pitting corrosion of type 301 stainless steel, *corrosion science*, **39**, pp 1665- 1672,1997.
- [10] Cruz, R.P., Nishikata A., & Tsuru T., Pitting corrosion mechanism of stainless steel under wet- dry exposure in chloride containing environments, *corrosion science*, **40**, pp 125-139, 1998.
- [11] Trethewey, K.T. & Chamberlain, J., Corrosion for science and engineering, 2nd edition, UK, 1995.



- [12] Jeffrey, R. and Melches, R., The changing topography of corroding mild steel surface in sew water, *Corrosion science*, **49**, pp 2270-2288, 2007.
- [13] Kim, DK., Muralidharan, S., Ha, T.H., Bae, J.H., Ha, Y.C., Lee, H.G. & Scandebury, JD., electrochemical studies on the alternating current corrosion of mild steel under cathodic protection in marine environments, *Electrochemical Acta*, **51**, pp 5259-5267, 2006.
- [14] AL-Fozan, S. & Umalik, A., Pitting behaviour of type 316L stainless steel in Arabian Gulf seawater technical report no. SWCC (RDC), 1992.
- [15] Abd El- Meguid, E., Mohmoud, N., and Gouda, A., Pitting corrosion behaviour of 316L in chloride containing solution, *British corrosion journal*, **33**, pp 42-48, 1998.
- [16] Chuan, M. and Tseng, W., Environmentally assisted cracking behaviour of single and dual phase stainless steel in hot chloride solution, *Materials chemistry and physics*, **84**, pp 162-170, 2004.
- [17] Refaey, S.A., Taha F. & Abd El- Malak, AM, Corrosion and inhibition of 316L stainless steel in neutral medium, *International Electrochem Society*, **1**, pp 80-91, 2006.

